A GeoSTAR Progress Report

B. H. Lambrigtsen, S. T. Brown, S. J. Dinardo, P. P. Kangaslahti, A. B. Tanner, W. J. Wilson
Jet Propulsion Laboratory – California Institute of Technology
Pasadena, CA

J. R. Piepmeier
Goddard Space Flight Center
Greenbelt, MD

C. S. Ruf, S. M. Gross, S. Musko, S. Rogacki
University of Michigan
Ann Arbor, MI

Abstract—**The Geostationary Synthetic Thinned Aperture Radiometer (GeoSTAR) is a new concept for a microwave sounder, intended to be deployed on NOAA's next generation of geostationary weather satellites, GOES-R. A ground based prototype has been developed at the Jet Propulsion Laboratory, under NASA Instrument Incubator Program sponsorship, and is now undergoing tests and performance characterization. With the aperture synthesis approach used by GeoSTAR it is possible to achieve very high spatial resolutions even in the crucial 50-GHz temperature sounding band without having to deploy the impractically large parabolic reflector antenna that is required with the conventional approach. The technology and system design required for GeoSTAR are rapidly maturing, and it is expected that a space demonstration mission can be developed before the first GOES-R launch. GeoSTAR will be ready for operational deployment 2-3 years after that. The prototype developed under IIP implements a small version of the temperature sounding component of GeoSTAR, is fully functional as a sounder and has all of the features and capabilities of an operational system with the exception of spatial resolution. It therefore represents a complete proof of concept as well as significant risk reduction for a space implementation.**

I. INTRODUCTION

The National Oceanic and Atmospheric Administration (NOAA) has for many years operated Polar-orbiting Operational Environmental Satellite systems (POES) in low-earth orbit (LEO), and Geostationary Operational Environmental Satellite systems (GOES) in geostationary earth orbit (GEO). The POES satellites have been equipped with both infrared (IR) and microwave (MW) atmospheric sounders, which together make it possible to determine the vertical distribution of temperature and humidity in the troposphere- even under cloudy conditions. In contrast, the GOES satellites have only been equipped with IR sounders. Geostationary MW sounders have not yet been feasible due to the large apertures required to achieve sufficient spatial resolution. As a result, and since clouds are almost completely opaque at infrared wavelengths, GOES soundings can only be obtained in cloud free areas and in the upper atmosphere, above the cloud tops. This has hindered the effective use of GOES data in numerical weather prediction. Full sounding capabilities with the GOES system is highly desirable because of the advantageous spatial and temporal coverage that is possible from GEO. While POES satellites provide coverage in relatively narrow swaths, and with a revisit time of 12-24 hours or more, GOES satellites can provide continuous hemispheric or regional coverage, making it possible to monitor highly dynamic phenomena such as hurricanes.

In response to a 2002 NASA Research Announcement calling for proposals to develop technology to enable new observational capabilities from geostationary orbits, the Geostationary Synthetic Thinned Aperture Radiometer (GeoSTAR) was proposed as a solution to the GOES MW sounder problem. GeoSTAR synthesizes a large aperture to measure the atmospheric parameters at microwave frequencies with high spatial resolution from GEO without requiring the very large and massive dish antenna of a real-aperture system. With sponsorship by the NASA Instrument Incubator Program (IIP), an effort is currently under way at the Jet Propulsion Laboratory to develop the required technology and demonstrate the feasibility of the synthetic aperture approach – in the form of a small ground based prototype. This is being done jointly with collaborators at the NASA Goddard Space Flight Center and the University of Michigan and in consultation with personnel from the NOAA/NESDIS Office of System Development. The objectives are to reduce technology risk for future space implementations as well as to demonstrate the measurement concept, test performance, evaluate the calibration approach, and assess measurement accuracy. When this risk reduction effort is completed, a space based GeoSTAR program can be initiated, which will for the first time provide MW temperature and water vapor soundings as well as rain mapping from GEO, with the same measurement accuracy and spatial resolution as is now available from LEO – i.e. 50 km or better for temperature and 25 km or better for water vapor and rain. Furthermore, the GeoSTAR concept makes it feasible to expand those capabilities without limit, to meet future measurement needs.

II. INSTRUMENT CONCEPT

As illustrated conceptually in Fig. 1, GeoSTAR consists of a Y-array of microwave receivers, which are operated in I/Q heterodyne mode (i.e. each receiver generates both a real and an imaginary IF signals). All of the antennas are pointed in the same direction. A digital subsystem computes cross-correlations between the IF signals of all receivers

simultaneously, and complex cross-correlations are formed between all possible pairs of antennas of the array. In the small-scale example of Fig. 1 there are 10 antennas and 45 complex correlations (=10*9/2). Each correlator and antenna pair forms an interferometer, which measures a particular spatial harmonic of the brightness temperature image across the field of view (FOV). The spatial harmonic depends on the spacing between the antennas and the wavelength of the radiation being measured. As a function of antenna spacing, the complex cross-correlation measured by an interferometer is called the visibility function. This function is essentially the Fourier transform of the function of brightness temperature versus incidence angle. By sampling the visibility over a range of spacings and azimuth directions one can reconstruct, or "synthesize," an image in a computer by discrete Fourier transform. These techniques are well known in radio astronomy, but are relatively new to earth remote sensing problems.

The "Y" configuration of the GeoSTAR array is motivated by the need to measure a complete set of visibility samples with a minimum number of antennas. In principle, one can measure the visibility function with just two antennas by mechanically varying their spacing and orientation. But this is not practical for the present application, and would require too much observation time for the sequential measurements. Instead, GeoSTAR uses a thinned (or "sparse") array to simultaneously measure all the required spacings from a fixed antenna geometry. There are many kinds of sparse arrays, and the "Y" array of Fig. 1 is one of the best in terms of efficient use of antennas and in terms of the simplicity of the structure - which lends itself well to a spaceborne deployment. As illustrated in Fig. 1, the spacings between the various antenna pairs yield a uniform hexagonal grid of visibility samples. By radio astronomy convention, the spacings are called the "baselines," with the dimensions "u" and "v." The primary advantage of the sparse array is that it uses far less physical antenna aperture space than the comparable real aperture.

The smallest spacing of the sample grid in Fig. 1 determines the unambiguous field of view, which for GeoSTAR must be larger than the earth disk diameter of 17.5° when viewed from GEO. This sets both the antenna spacing and diameter at about 3.5 wavelengths, or 2.1 cm at 50 GHz, for example. The longest baseline determines the smallest spatial scale that can be resolved. To achieve a 50 km spatial resolution at 50 GHz, a baseline of about 4 meters is required. This corresponds to approximately 100 receiving elements per array arm, or a total of about 300 elements. This in turn results in about 30,000 unique baselines, 60,000 uv sampling points (given conjugate symmetry), and therefore 60,000 independent pixels in the reconstructed brightness temperature image.

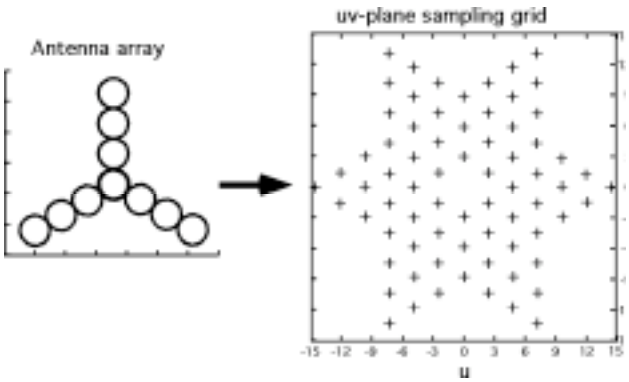

Fig. 1. Antenna array and UV samples

III. PROTOTYPE

A small-scale prototype has been built to address the major technical challenges facing GeoSTAR. These challenges are centered around the issues of system design and calibration. (Power consumption has also been a major concern, but recent and continuing miniaturization of integrated circuit technology has demonstrated that this should no longer be seen as a major issue.) Synthesis arrays are new and untested in atmospheric remote sensing applications, and the calibration poses many new problems, including those of stabilizing and/or characterizing the phase and amplitude response of the antenna patterns and of the receivers and correlators. System requirements need to be better understood - and related to real hardware. To these ends the prototype was built with the same receiver technology, antenna design, calibration circuitry, and signal processing schemes as are envisioned for the spaceborne system. Only the number of antenna elements differ. Progress on this system has been rapid in recent months, and the following discussion will attempt to emphasize the most recent achievements at the time of writing.

The prototype consists of a small array of 24 elements operating with 4 AMSU channels between 50 and 54 GHz. Fig. 2 shows a photo of the prototype, which has already evolved considerably from the earlier concept of Fig. 1. One change evident in Fig. 2 concerns the basic layout of the Y array: note that in contrast with Fig. 1 there is no single horn at the center of the array. The center horn posed a number of unnecessary complications to the system, related to the physical package (there is not enough room) and the electrical design (to be discussed below). The solution is to remove the one horn from the center of the array, stagger the

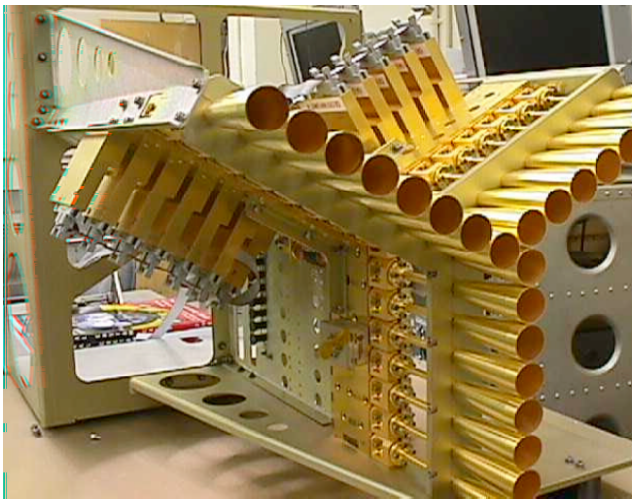

Fig 2. GeoSTAR prototype

three arms counter clockwise, and then bring them together so that the three innermost horns form an equilateral triangle. This staggered-Y configuration eliminates the need for an odd receiver at the center, which simplifies both mechanical and electronic design. The only penalty is a slight and negligible loss of visibility coverage.

A simplified block diagram of the GeoSTAR prototype is given in Fig. 3. From left to right in Fig. 3 - or from front to back in Fig. 2 - the signal starts at the horn aperture with a vertical polarization, and then passes through a waveguide twist which aligns the waveguide to the orientation of the 8-element array arm. Each of the three arms require different twists: the top two arms of Fig. 2 twist 60° in opposite directions, and the bottom arm doesn't twist at all. This results in all receivers detecting the same linear polarization, as is commonly required for sounders with channels sensitive to surface radiation (which is polarized). GeoSTAR is very sensitive to antenna pattern differences among antennas, and a waveguide twist proved to be the easiest solution to guarantee a precise polarization match.

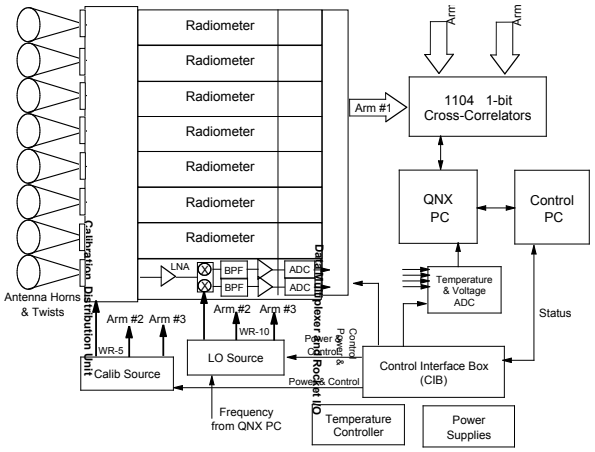

Fig 3. Receiver system block diagram – one of three arms shown

The signal in Fig. 3 then passes through an 8-way calibration feed which periodically injects a noise signal into all receivers from a common noise diode source. This signal will be used as a reference to stabilize the system against gain, phase, and system noise drifts. The injected noise signal needs to be in the range of 1 to 10 K of equivalent noise temperature at the receiver input.

The noise diode signal is distributed to the three arms via phase shifters. Each of these phase shifters consists of a PIN diode and hybrid MMIC assembly which can switch between 0° and 120°. Correlations that occur between receivers of different arms can be excited by the noise diode with three possible phases using any two of these switches. This capability is critical to ensure that every correlator can be stabilized with respect to both phase and amplitude. Without this capability one must otherwise depend on perfect quadrature balance of the complex correlations, which is predictably not perfect. It is also worth noting that the phase of the noise diode cannot be shifted among the 8 antennas of a given arm, but that such a capability is not needed for the staggered-Y arrangement of the antennas. With the staggered-Y all correlations within an arm represent visibility samples that are redundant to samples that can otherwise be obtained between elements of different arms. These redundant correlations are not needed for image reconstruction, so they do not need to be calibrated.

Continuing the discussion of Fig. 3, the antenna signal passes into the MMIC receiver module, where it is amplified using InP FET low noise amplifiers and then double-sideband downconverted in phase quadrature by subharmonic mixers to two IF signals of 100 MHz bandwidth. The bandwidth is defined by lumped element filters. A photograph of a prototype receiver module is provided in Fig. 4. The local oscillator operates from 25 to 30 GHz, and is distributed via three phase shifters. These MMIC phase shifters periodically shift the phase of each arm by 90° (180° at RF) to provide a means of switching the correlator phase and chopping out correlator biases.

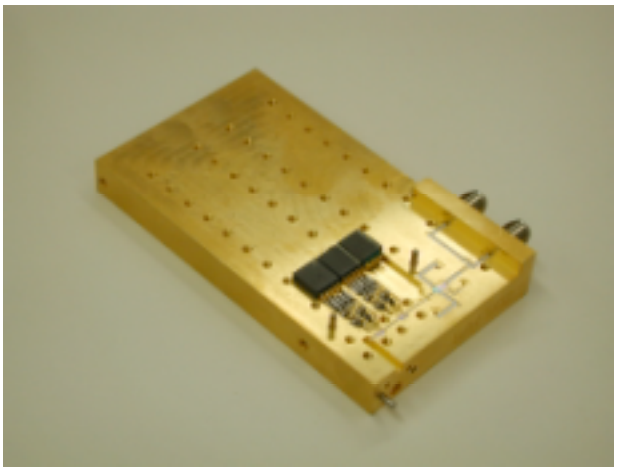

Fig. 4. Prototype receiver module – cover removed

Again, the staggered-Y arrangement of the array proves crucial to this function since one would otherwise need phase shifters within each arm. (This was the original plan, but it proved impractical due to the timing complexity when switching phase among all 24 receivers.)

The in-phase (I) and quadrature (Q) IF signals from each receiver are then digitized at a clock rate of 110 MHz. For reasons of product availability, the analog to digital converter is presently an 8-bit device, but this could be replaced with a two-bit or possibly just a one-bit converter to save power. The correlations only require 1-bit resolution (i.e. the sign bit), and the extra bits are only used to monitor changes in system noise temperature. There is a single multiplexer for each arm of the array - the term "multiplexer" here refers to the fact that eight receivers are combined on a single digital bus for transmission to the central correlator. An FPGA performing most of the functions of the multiplexer also includes "totalizers", which are used to count the occurrences of each ADC output state so that the threshold levels can be compared with the known Gaussian statistics of the IF voltage.

Perhaps the most important subsystem is the correlator, which must perform multiplications of all 100-MHz signal pairs in real time. For a spaceborne operational system with 100 elements per arm discussed earlier, that requires on the order of 20 trillion multiplications per second. To achieve such a high processing rate with a reasonable power consumption, the correlators are implemented as 1-bit digital multiply-and-add circuits using a design developed by the University of Michigan. 1-bit correlators are commonly used in radio astronomy. The correlator for the GeoSTAR prototype, where low cost was more important than low power consumption, is implemented in FPGAs. An operational system will use low-power application specific integrated circuits (ASICs). Current state of the art would then result in a power consumption of less than 20 W for the 300-element system discussed above, and per Moore's Law this will decline rapidly in future years.

IV. EARLY TEST RESULTS

The initial tests of the correlator simply involved running the whole system in the lab with no particular target. The totalizer thresholds were all adjusted so that the counts for an ambient brightness temperature were distributed with approximately 10 % below the negative "-3" threshold, 40% between "-3" and the zero threshold, and 40% and 10% for the symmetric positive voltage totalizers.

Fig. 5 plots a sample of totalizer data collected just after the system was powered up. The net fraction of counts beyond the "+/-3" thresholds are plotted for the I and Q digitizers of two example channels (receivers 5 and 17). The upward trend in this plot is due to the fact that the receivers are warming up, and the rectangular step in the middle corresponds to a person standing in front of the antenna for about 20 seconds. This represents about 10 to 20 K of noise signal and can be used to roughly estimate the radiometric

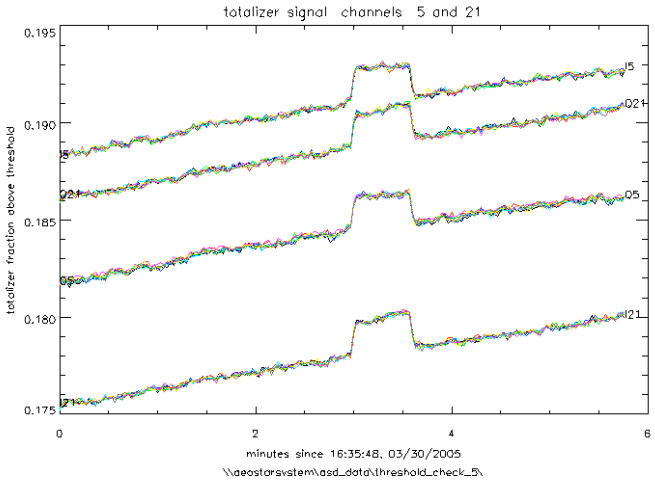

Fig. 5. Digitized output (totalizer count above a threshold) for two receivers Different colors represent different LO phase states

sensitivity of the receivers. As we can see, the gain drift is quite large. Presumably, if the system was fully warmed up, the totalizer fraction plotted here would settle to the approximate 20% target that was set into the thresholds, and this drift is no cause for concern. In fact, we see a reasonable radiometric response in this plot. We do not expect that these totalizer power measurements are important to the overall calibration, but it was encouraging to see the response. Fig. 5 also includes the effect of rapidly switching the LO phase – an important part of the GeoSTAR phase calibration system – and very little difference is apparent in these plots (another encouraging finding). The phase is switched according to Table I.

TABLE I
LO PHASE STATES

LO state	Arm #1	Arm #2	Arm #3
1	0°	0°	0°
2	0°	0°	-95.09°
3	0°	-89.64°	-138.65°
4	0°	-89.64°	-47.63°
5	0°	-61.78°	-47.63°
6	0°	-61.78°	-138.65°
7	0°	-149.18°	-95.09°
8	0°	-149.18°	0°

The operation of the phase switch is perhaps best illustrated with real data. Fig. 6 provides two examples of the raw correlations measured in a recent test with a noise diode placed in front of the GeoSTAR array. The noise diode was on at the beginning, and turned off near the end. As in Fig. 5, the colors here correspond to the different phase switch states of Table I. In Fig. 6a, which is a correlation from arms #1 and #2, the correlations shift to precisely four

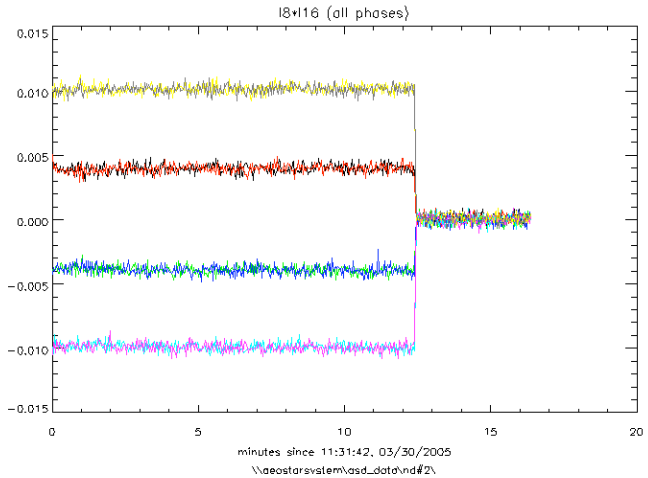

a) Two receivers from arms 1 and 2

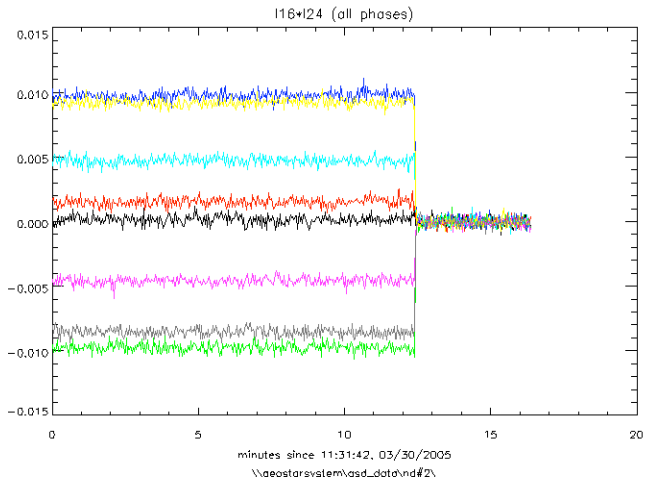

b) Two receivers from arms 2 and 3

Fig. 6. Examples of raw correlator responses to a noise diode source

levels. These match the four phases listed under "arm #2" of Table I. It is encouraging that the arm#3 phase switch does not have any effect on these data, which shows that the isolation between phase shifters is good and that there is minimal cross-contamination of the different phase switches. In Fig. 6b, on the other hand, there are eight distinct responses in the correlation formed between arms #2 and #3, as predicted from Table 1.

In all correlators, the known LO phases from Table I are used in a least squares solution to estimate a magnitude and phase for every individual correlator. The essence of this least squares fit is illustrated in Fig. 7, which plots raw correlations versus LO phase for all four correlators represented in Fig. 6b along with the sine waves that have been fit to the data. The retrieved parameters are magnitudes and phases of the sine waves, and the null-offsets. It can be seen that the data points of Fig. 7 fit the regression very well. The retrieved magnitudes and phases of these four correlators are also plotted in Fig. 8, and we see excellent agreement here as well. This all indicates that the correlators are very well matched and are operating with good efficiency. In Fig. 8, the I*Q and Q*I phases have been offsets by +90° and -90°, respectively, and we see only about 5° of disagreement between these quadrature correlations, which is excellent considering their dependence on the quadrature mixer hardware.

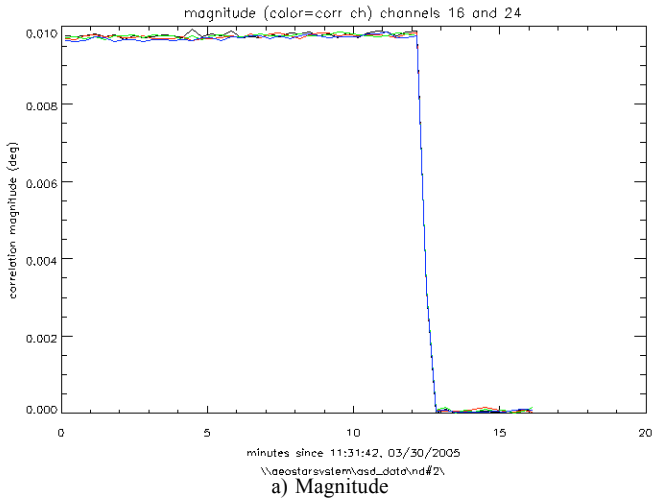

a) Magnitude

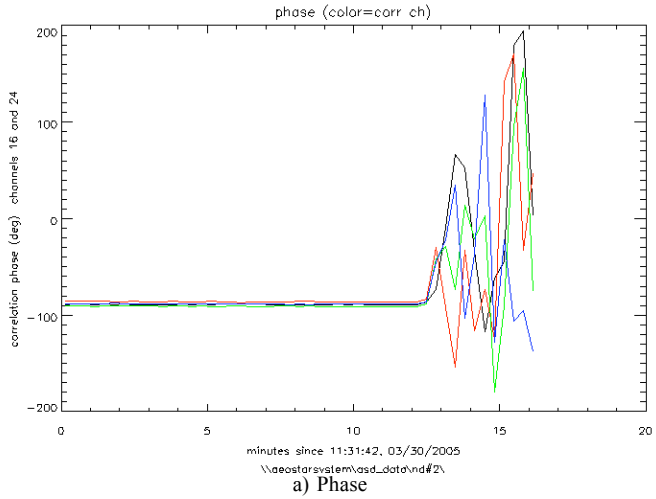

a) Phase

Fig. 8. Retrieved magnitude and phase from the noise source correlations

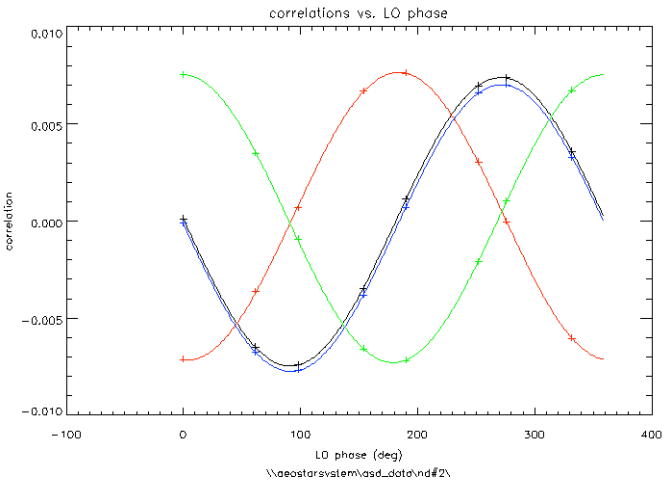

Fig. 7. Measured correlations vs. LO phase with sinusoidal fit functions

Following the laboratory tests, the system was moved outdoors to observe the sky and the sun. The array was pointed into the path of the sun, and the sun was allowed to pass the center of the field of view at an elevation of 45°. Pictures of the basic setup are shown in Fig. 9. During these tests, the antenna fixture was disturbed several times as different sun shields were arranged on the structure to keep the receivers from overheating in the sun, as shown.

a) Initial configuration

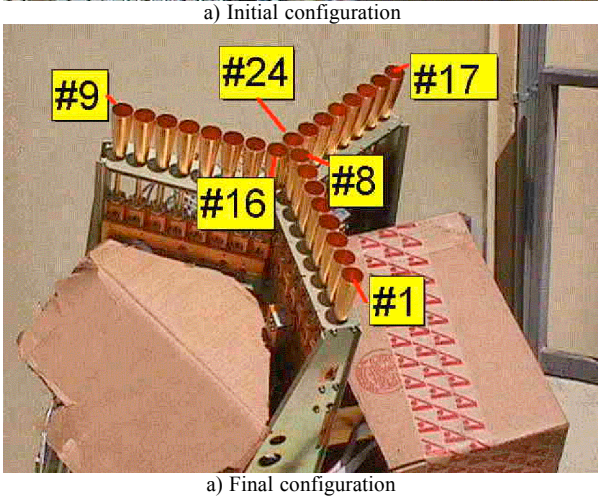

a) Final configuration

Fig. 9. GeoSTAR prototype outdoors to observe the sun's transit

This activity resulted in several interruptions in the data,

and it can be expected that the uneven temperatures of the antennas resulted in uneven receiver noise temperatures. Although none of the calibration subsystems were operated during this test (except the LO phase switching), the results were spectacular and give us confidence that both system design and performance will exceed expectations.

Fig. 10 shows the raw correlations and the retrieved magnitude and phase for one sample baseline during the solar transit. The glitches caused by the mechanical disturbances discussed above are obvious. Nevertheless, the results are very satisfactory. We have done some further analysis of the solar data, and Fig. 11 shows a series of reconstructed (but uncalibrated) brightness temperature images. (An animation of the entire sequence also exists.)

These images were reconstructed using the so-called G-matrix approach and accounts for the elemental antenna patterns. The most notable feature in these images is the hexagonal-symmetric sidelobe pattern. Fig. 12 shows a contour plot of this pattern, derived from the observations when the sun was near the center of the FOV as well as a line plot along a particular azimuth direction. The most notable feature here is that the pattern is indistinguishable from the theoretical "sinc" function. In particular, note that the sidelobes are both positive and negative. That makes it possible to apply image processing techniques to achieve an optimal balance of image sharpness (i.e. spatial resolution) and beam efficiency (i.e. effective sidelobe level). This is one of the most powerful features of an aperture synthesis system such as GeoSTAR.

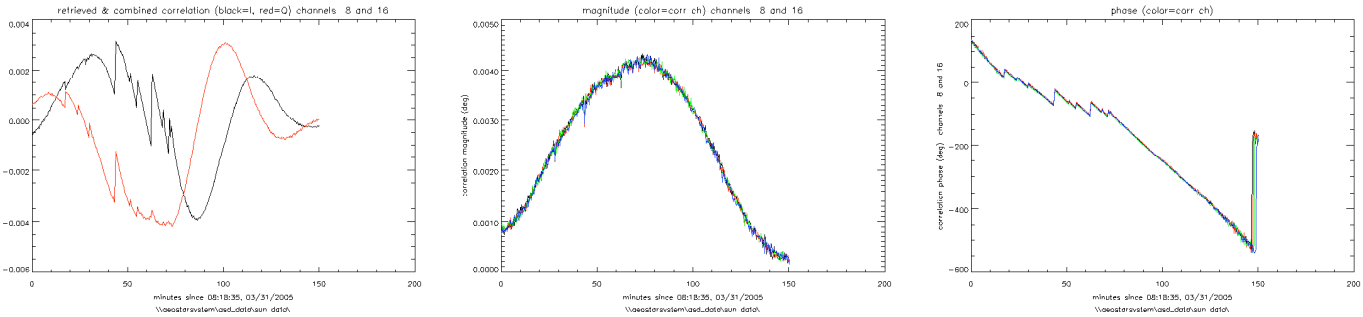

a. Raw correlations b. Derived magnitude Derived phase

Fig. 10. Sun measurements: One neighboring receiver pair near the center of the array

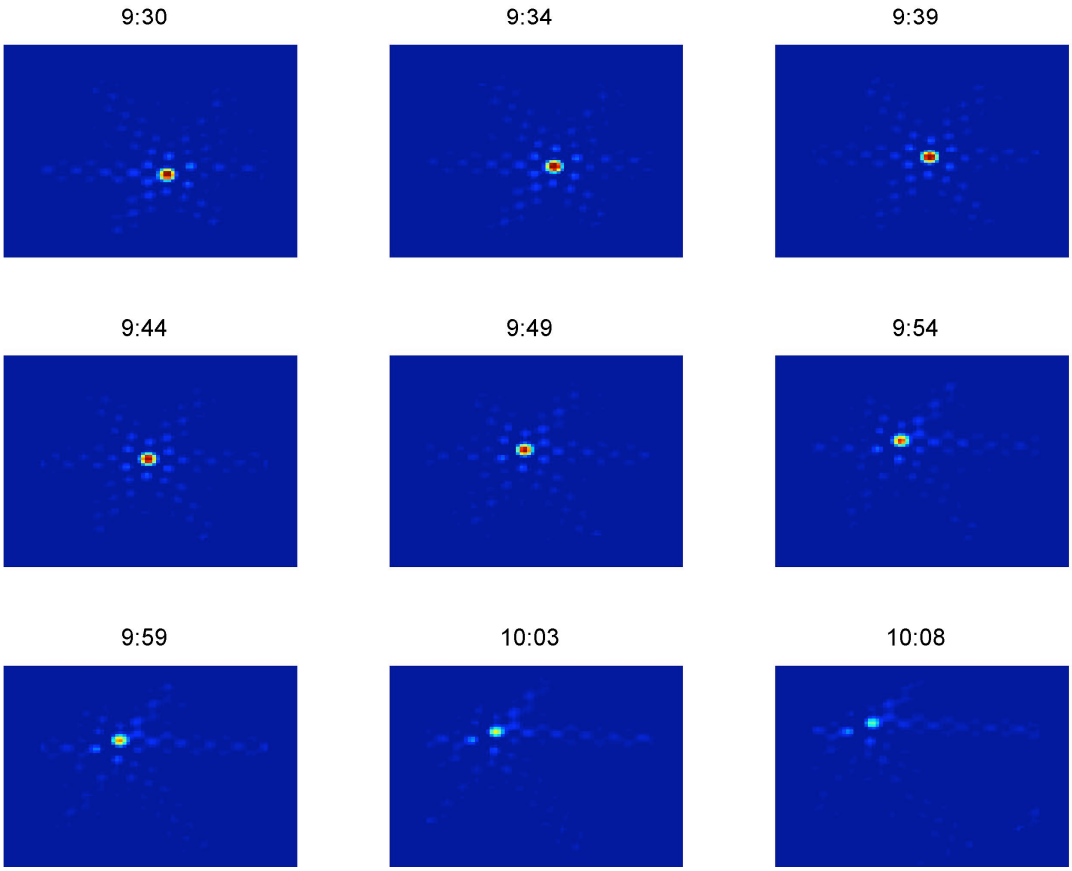

Fig. 11. GeoSTAR images of solar transit (times are in PDT)

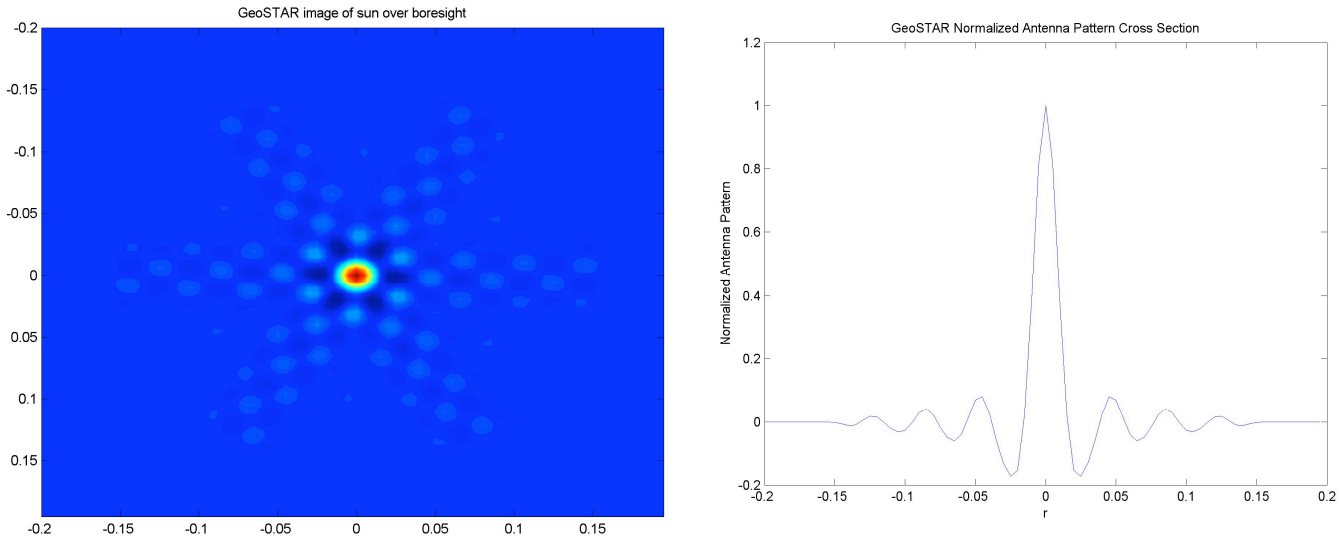

Fig. 12. GeoSTAR raw antenna pattern

V. CONCLUSIONS

The GeoSTAR prototype construction is nearly complete, but very promising measurements have already been made that indicate excellent performance. In the coming months we will activate the various calibration subsystems and complete the proof of concept that has been our main objective. Our efforts are focused on building a practical low power system which will form the basis of a future spaceborne system. We are very carefully examining error budgets, and hope to demonstrate a comprehensive and well justified system calibration based on real hardware.

ACKNOWLEDGMENTS

This work was carried out at the Jet Propulsion Laboratory, California Institute of Technology under a contract with the National Aeronautics and Space Administration and at the University of Michigan Space Physics Research Lab under a contract with the NASA Goddard Space Flight Center. We acknowledge the invaluable support of Mary Wells, April Campbell, William Imbriale, Baron Latham, Chi Truong and Dennis Harding at JPL as well as others at U. Michigan and GSFC too numerous to mention by name.